

Dependence of the Frequency of the KiloHertz Quasi-Periodic Oscillations on X-ray Count Rate and Colors in 4U 1608–52

M. Méndez^{1,2}, M. van der Klis¹, E. C. Ford¹, R. Wijnands¹, J. van Paradijs^{1,3},

ABSTRACT

We present new results based on observations carried out with the *Rossi X-ray Timing Explorer* during the decay of an outburst of the low-mass X-ray binary (LMXB) and atoll source 4U 1608–52. Our results appear to resolve, at least in 4U 1608–52, one of the long-standing issues about the phenomenology of the kilohertz quasi-periodic oscillations (kHz QPOs), namely, the lack of a unique relation between the frequency of the kHz QPOs and the X-ray flux. We show that despite its complex dependence on the X-ray flux, the frequency of the kHz QPOs is monotonically related to the position of the source in the color-color diagram. Our findings strengthen the idea that, as in the case of Z sources, in the atoll sources the X-ray flux is not a good indicator of \dot{M} , and that the observed changes in the frequency of the kHz QPOs in LMXBs are driven by changes in \dot{M} . These results raise some concern about the recently reported detection of the orbital frequency at the innermost stable orbit in 4U 1820–30.

Subject headings: accretion, accretion disks — stars: neutron — stars: individual (4U 1608–52) — X-rays: stars

¹Astronomical Institute “Anton Pannekoek”, University of Amsterdam and Center for High-Energy Astrophysics, Kruislaan 403, NL-1098 SJ Amsterdam, the Netherlands

²Facultad de Ciencias Astronómicas y Geofísicas, Universidad Nacional de La Plata, Paseo del Bosque S/N, 1900 La Plata, Argentina

³Physics Department, University of Alabama in Huntsville, Huntsville, AL 35899, USA

1. Introduction

Nearly three years have elapsed since the first kilohertz quasi-periodic oscillations (kHz QPOs) were discovered with the *Rossi X-ray Timing Explorer* (RXTE) in the X-ray flux of Scorpius X-1 (van der Klis et al. 1996) and 4U 1728-34 (Strohmayer, Zhang, & Swank 1996). In the meantime, kHz QPOs have been observed in the persistent flux of 18 low mass X-ray binaries (LMXBs; see van der Klis 1998 for a review), both in the so called Z sources and in the atoll sources (Hasinger & van der Klis 1989, hereafter HK89). Except in Aql X-1, which showed a single kHz peak in its power spectrum (Zhang et al. 1998a), in the other 17 sources two simultaneous kHz QPO peaks have been observed. In some sources a third, nearly-coherent, QPO peak has been detected during type-I X-ray bursts, with a frequency which was consistent with being equal to one or two times the frequency separation of the kHz QPOs observed in the persistent flux (Strohmayer, Swank, & Zhang 1998). It was suggested that a beat frequency mechanism is responsible for this commensurability in the QPO frequencies (Strohmayer et al. 1996; Miller, Lamb & Psaltis 1998), but this interpretation is not without problems (van der Klis et al. 1997; Méndez et al. 1998c; Méndez, van der Klis, & van Paradijs 1998b).

The dependence of the kHz QPO frequencies on X-ray luminosity, which is usually assumed to be a measure of the mass accretion rate, is complex. While in a given source, on a time scale of hours, there is a good correlation between frequency and luminosity, sources that span nearly three orders of magnitude in luminosity, such as Sco X-1 and 4U 0614+09, show kHz QPOs that cover the same range of frequencies (van der Klis 1997). It is as if the frequency of the kHz QPO depends on the difference between instantaneous and average luminosity in each source rather than on the luminosity itself.

A similar effect is seen between observations of the same source at different epochs. On time scales of hours, frequency and X-ray flux are well correlated, but between different epochs the source covers the same range of frequencies even if the average flux is different by 40 % or more (e.g., Aql X-1; Zhang et al. 1998a).

In this paper we present new results that appear to resolve the latter of these two issues, at least in 4U 1608-52. We show that while on time scales longer than ~ 1 day the frequency of the kHz QPOs is not

well correlated to the X-ray flux, it is very well correlated to the position of the source in the color-color diagram. From this result we conclude that the observed changes in the frequency of the kHz QPOs in 4U 1608-52 are driven by changes in the mass accretion rate, and that the lack of correlation between QPO frequency and X-ray count rate occurs because, as in the case of the Z sources, in atoll sources there is no one-to-one relationship between the observed X-ray flux and the mass accretion rate.

2. Observations and Results

All the observations presented here were obtained using the proportional counter array (PCA) onboard RXTE. We include the data of the decay of the 1996 outburst (Berger et al. 1996; Méndez et al. 1998a), and of the 1998 outburst (Méndez et al. 1998c; Fig. 1 there shows a light curve of the 1998 outburst.) The observations as well as the modes used to record the data are described in Méndez et al. (1998c). We also include here a recent Public Target of Opportunity RXTE/PCA observation of ~ 7.3 ks performed on August 6 1998, 03:13 UTC. The observing modes for this last observation were similar to those used by Méndez et al. (1998c) after 1998 March 27.

We calculated count rates in 5 energy bands, 2.0 – 3.5 – 6.4 – 9.7 – 16.0 keV, and 2.0 – 16.0 keV, taking into account the gain changes applied to the PCA in March and April 1996. In a few of the observations one or two of the five detectors of the PCA were switched off; we only used the three detectors which were always on to calculate these count rates. We subtracted the background contribution in each band using the standard PCA background model version 2.0c⁴, and normalized the count rates to 5 detectors.

In Figure 1 we show a color-color diagram of 4U 1608-52. This is the first time that 4U 1608-52 is observed to move across all the branches of the atoll, and constitutes one of the best examples of the color-color diagram of an atoll source. Based on this diagram we conclude that in 1996, as the source count rate decreased, 4U 1608-52 gradually moved from the lower part of the banana to the island state. In 1998, at the peak of the outburst, 4U 1608-52 was in the upper part of the banana, and gradually moved down to the lower part of the banana and the island state as

⁴The PCA Background Estimator is available at <http://lhea-www.gsfc.nasa.gov/users/stark/pca/pcabackest.html>, which is maintained by NASA/GSFC.

the count rate decreased. In general, the count rate is observed to increase along the track from the island state to the banana branch, but the relation between count rate and either of the two colors is much less clean than that between colors.

The high-time resolution data confirm this preliminary state classification. We divided the 2 – 60 keV data into segments of 256 s and 512 s, and calculated power spectra up to a Nyquist frequency of 2048 Hz, normalized to fractional rms squared per Hertz. The characteristics of the $\lesssim 100$ Hz part of these power spectra changed in correlation with the position of the source in the color-color diagram. When 4U 1608–52 was in the upper and lower parts of the banana, the power spectra fitted a power law below ~ 1 Hz (the Very Low Frequency Noise, VLFN), and an exponentially cut-off power law above ~ 1 Hz (the High Frequency Noise, HFN; see HK89). As 4U 1608–52 moved from the upper to the lower parts of the banana, the fractional amplitude of the VLFN (0.001 – 1 Hz) decreased from $\sim 6\%$ rms to $\sim 2\%$ rms, while the fractional amplitude of the HFN (1 – 100 Hz) increased from $\sim 1\%$ rms to $\sim 5\%$ rms. In the island state the VLFN disappeared completely (the 95% confidence upper limits were $\sim 1\%$ rms), and the amplitude of the HFN increased further to $\sim 10 - 17\%$ rms. (A more detailed analysis of the low frequency part of the power spectra will be presented elsewhere.)

The $\gtrsim 100$ Hz part of the power spectra also changed in correlation with the position of the source in the color-color diagram: we only observed kHz QPOs when 4U 1608–52 was at certain positions of the color-color diagram (see Fig. 1). For those segments where we observed QPOs, the 2 – 60 keV fractional amplitudes of the lower-frequency and higher-frequency, hereafter the lower and upper QPO, varied from 5.3% to 9.1% rms, and from 3.3% to 8.8% rms, respectively. We did not detect kHz QPOs in the upper part of the banana, with 95% confidence upper limits of 0.8% to 4.6% rms depending on the source count rate and the assumed width of the QPO, nor in the extreme island state (upper right corner of the color-color diagram), with 95% confidence upper limits of 3.5% to 10% rms. While these upper limits strongly suggest the absence in the upper banana of kHz QPOs as strong as those observed in the lower banana and the island states, we cannot rule out the presence of such kHz QPOs in the extreme island state, when the count rates were lowest.

To further characterize the dependence of the kHz

QPOs on other source parameters, we selected only those data where we detected two simultaneous kHz QPO peaks in the power spectrum (see Méndez et al. 1998c), so that the identification of the observed kHz peaks is unambiguous. We divided the data in segments of 64 s and produced a power spectrum for each segment extending from 1/64 Hz to 2048 Hz. In Figure 2 we show the dependence of the frequency of the lower QPO, ν_{low} , as a function of count rate for 4U 1608–52. This figure shows several branches, which reflect the relation between ν_{low} and count rate during individual observations that span from \sim half an hour to ~ 8 hours. The only exception is the branch at the lowest count rate where two different observations taken 8 days apart overlap. This figure clearly shows that while on time scales of a few hours or less ν_{low} is well correlated to count rate, on time scales greater than ~ 1 day the relation is complex and ν_{low} is not uniquely determined by the count rate. We obtained the same result using the 2 – 60 keV source flux instead of the count rate.

There is a much better correlation between ν_{low} and the position of the source on the color-color diagram. In Figure 3 we show ν_{low} as a function of hard color (see Fig. 1) for the same intervals shown in Figure 2. The complexity seen in the frequency vs. count rate diagram (Fig. 2) is reduced to a single track in the frequency vs. hard color diagram. The frequency of the lower kHz QPO increases as the hard color decreases, i.e., as 4U 1608–52 moves from the island state to the lower banana, and keeps increasing at the turn of the lower banana, where the hard color reaches its lowest value of ~ 0.40 .

The shape of the track in Figure 3 suggests that the hard color may not be sensitive to changes of state when the source moves into the banana in the color-color diagram. To further investigate this, we applied the S_z parameterization (e.g., Wijnands et al. 1997b), which we call S_a for atoll sources, to the color-color diagram. In this phenomenological approach we approximated the shape of the color-color diagram with a spline (Fig. 1), and we used the parameter S_a to measure positions along this spline. We set S_a to 1 at (2.67, 0.77), and to 2 at (2.19, 0.42), as indicated in Figure 1. We measured the position on the color-color diagram of each of the 64-s segments. We then grouped these segments into 36 sets, such that within each set ν_{low} did not vary by more than ~ 25 Hz, and the source count rate did not vary by more than 10%. (This is to avoid mixing segments that come

from different branches in Figure 2.) For each set we calculated the average frequency of the lower and upper kHz QPO peak, and of S_a . In Figure 4 we plot the frequencies of both kHz QPOs as a function of S_a . The error bars are the standard deviation of each selection. We also include in this figure several extra sets (open squares) for which we only detected one of the kHz QPOs, which therefore we could not a priori identify as the upper or lower peak. As expected, S_a is more sensitive than the hard color to changes of state when the source moves from the island state into the turn of the banana: S_a increases from ~ 2.04 to ~ 2.15 there, while the hard color saturates at ~ 0.40 . Figure 4 confirms that the frequency of the kHz QPOs is strongly correlated to the position of the source in the color-color diagram. It also shows that the steep rise of kHz QPO frequency at the turn of the lower banana is not just due to a lack of sensitivity of the hard color to state changes in this part of the color-color diagram, but that it occurs as a function of the position in the color-color diagram as well.

3. Discussion

Previous observations of kHz QPOs in atoll sources have resulted in a confusing picture concerning the dependence of QPO frequency on mass accretion rate. Cases have been reported where, in a given source, QPO frequency showed a good correlation to count rate or spectral hardness (Ford, van der Klis, & Kaaret 1998a; Wijnands et al. 1997c; Wijnands et al. 1998; Ford et al. 1998b; Zhang et al. 1998b; Wijnands & van der Klis 1997). In other cases, a correlation with count rate or flux was conspicuously lacking (Ford et al. 1997; Méndez et al. 1998a; Zhang et al. 1998a).

Our observations show for the first time that a total lack of correlation between frequency and count rate on time scales longer than a day (Fig. 2) can coexist with a very good correlation between frequency and position in the X-ray color-color diagram (Fig. 3). The frequency increases with S_a , as the source moves from the island to the banana. Only on time scales of hours does the QPO frequency appear to also correlate well with count rate. The presence of the QPOs also correlates well with the position in the color-color diagram: the QPOs are only detected in the lower banana and the moderate island states, and disappear both in the upper banana and in the extreme island states (Fig. 1).

In atoll sources \dot{M} is thought to increase monotonically with S_a along the track in the color-color diagram, from the island to the upper banana (HK89), whereas X-ray count rate tracks \dot{M} much less well (van der Klis et al. 1990; van der Klis 1994; Prins & van der Klis 1997). The properties of the < 100 Hz power spectra depend monotonically on inferred \dot{M} (HK89). Our result that the frequency of the kHz QPO is well correlated to S_a , but not to X-ray count rate, implies that in 4U 1608–52 the kHz QPO frequency *also* depends monotonically on inferred \dot{M} . By extension this conclusion applies to each atoll source; in Z sources similar conclusions were previously also reached (e.g., Wijnands et al. 1997a). Our analysis, however, sheds no light on the question why sources with very different inferred \dot{M} (e.g., 4U 0614+09 and Sco X–1) can have kHz QPO in the same range of frequencies.

Further indications for this interpretation come from the simultaneous analysis of the low and high frequency parts of the power spectra of other atoll sources. In 4U 1728–34 the kHz QPO frequencies were recently found to be very well correlated to several < 100 Hz power spectral properties (Ford & van der Klis 1998), and Psaltis, Belloni and van der Klis (1998) obtained a similar result for a number of other atoll (and Z) sources. In all these sources, not only the position in the color-color diagram and the various low frequency power spectral parameters, but also the frequencies of the kHz QPOs are all well correlated with each other. This indicates that the single parameter, inferred to be \dot{M} , which governs all the former properties also governs the frequency of the kHz QPO.

X-ray intensity is the exception: it can vary more or less independently from the other parameters. In 4U 1608–52, it can change by a factor of ~ 4 (see Fig. 2) while the other parameters do not vary significantly. If as inferred, this constancy of the other parameters means that \dot{M} does not change, then this indicates that strongly variable beaming of the X-ray flux, or large-scale redistribution of some of the radiation over unobserved energy ranges is occurring in order to change the flux by the observed factors, *without* any appreciable changes in the X-ray spectrum. We may need to scrutinize more closely the concept of \dot{M} in order to solve this dilemma. For example, perhaps the \dot{M} governing all the other parameters is the \dot{M} through the inner accretion disk, whereas matter also flows onto the neutron star in a more radial

inflow, or away from it in a jet.

In 4U 1608–52 we observe no evidence for a saturation of the frequency of the kHz QPOs at a constant maximum value as \dot{M} increases, different from what Zhang et al. (1998b) inferred for 4U 1820–30. They presented data in which the kHz QPO frequencies increase with count rate up to a threshold level, above which the frequencies remain approximately constant while the count rate keeps increasing. Interpreting count rate as a measure for \dot{M} they argue that this is evidence for the inner edge of the disk reaching the general-relativistic innermost stable orbit. However, we have shown here that, at least in 4U 1608–52, count rate is not a good measure for \dot{M} . Inspection of Figure 2 suggests that with sparser sampling our plot could easily have looked similar to the one presented by Zhang et al. (1998b) for 4U 1820–30. It will therefore be of great interest to see if in 4U 1820–30 the saturation of QPO frequency as a function of count rate is still there when this parameter is plotted as a function of position in the X-ray color-color diagram.

This work was supported in part by the Netherlands Organization for Scientific Research (NWO) under grant PGS 78-277 and by the Netherlands Foundation for research in astronomy (ASTRON) under grant 781-76-017. MM is a fellow of the Consejo Nacional de Investigaciones Científicas y Técnicas de la República Argentina. JVP acknowledges support from the National Aeronautics and Space Administration through contract NAG5-3269, 5-4482 and 5-7382. This research has made use of data obtained through the High Energy Astrophysics Science Archive Research Center Online Service, provided by the NASA/Goddard Space Flight Center.

REFERENCES

- Berger, M. et al. 1996, *apJ*, 469, L13
- Ford, E., et al. 1997, *ApJ*, 475, L123
- Ford, E. & van der Klis, M. 1998, *ApJ*, 506, L39
- Ford, E., van der Klis, M., & Kaaret, P. 1998a, *ApJ*, 498, L41
- Ford, E. C., van der Klis, M., van Paradijs, J., Méndez, M., Wijnands, R., & Kaaret, P. 1998b, *ApJ*, 508, L105
- Hasinger, G., & van der Klis, M. 1989, *A&A*, 225, 79 (HK89)
- Méndez, M., et al. 1998a, *ApJ*, 494, L65
- Méndez, M., van der Klis, & van Paradijs, J. 1998b, *ApJ*, 506, L117
- Méndez, M., van der Klis, M., Wijnands, R., Ford, E. C., van Paradijs, J., & Vaughan, B. A. 1998c, *ApJ*, 505, L23
- Miller, M. C., Lamb, F. K., Psaltis, D. 1998, *ApJ*, in press (astro-ph/9609157)
- Prins, S., & van der Klis, M. 1997, *A&A*, 319, 498
- Psaltis, D., Belloni, T., van der Klis, M. 1998, in preparation
- Strohmayer, T. E., Swank, J. H., & Zhang, W. 1998, in *The Active X-Ray Sky: Results from BeppoSAX and Rossi-XTE*, ed. L. Scarsi, H. Bradt, P. Giommi, & F. Fiore (Amsterdam: Elsevier Science), 129
- Strohmayer, T. E., Zhang, W., & Swank, J. H. 1996, *IAU Circ.* 6320
- van der Klis, M. 1994, *ApJS*, 92, 511
- van der Klis, M. 1997, in *Ap&SS Library*, Vol. 128, *Astronomical Time Series*, ed. D. Maoz, A. Sternberg, & E. M. Leibowitz (Dordrecht: Kluwer Academic Publishers), 121
- van der Klis, M. 1998, in *NATO ASI Series C*, Vol. 515, *The many faces of Neutron Stars*, ed. R. Buccheri, J. van Paradijs, & M.A. Alpar (Dordrecht: Kluwer), 337
- van der Klis, M., Hasinger, G., Damen, E., Penninx, W., van Paradijs, J., & Lewin, W. H. G. 1990, *ApJ*, 360, L19
- van der Klis, M., Swank, J. H., Zhang, W., Jahoda, K., Morgan, E., Lewin, W. H. G., Vaughan, B. A., & van Paradijs, J. 1996, *IAU Circ.* 6319
- van der Klis, M., Wijnands, R. A. D., Horne, K., & Chen, W. 1997, *ApJ*, 481, L97
- Wijnands, R., et al. 1997a, *ApJ*, 490, L157
- Wijnands, R. A. D., & van der Klis, M. 1997, *ApJ*, 482, L65
- Wijnands, R. A. D., van der Klis, M., Kuulkers, E., Asai, K., & Hasinger, G. 1997b, *A&A*, 323, 399
- Wijnands, R., van der Klis, M., Méndez, M., van Paradijs, J., Lewin, W. H. G., Lamb, F. K., Vaughan, B. A., & Kuulkers, E. 1998, *ApJ*, 495, L39
- Wijnands, R. A. D., van der Klis, M., van Paradijs, J., Lewin, W. H. G., Lamb, F. K., Vaughan, B. A., & Kuulkers, E. 1997c, *ApJ*, 479, L141
- Zhang, W., Jahoda, K., Kelley, R. L., Strohmayer, T. E., Swank, J. H., & Zhang, N. 1998a, *ApJ*, 495, L9
- Zhang, W., Smale, A. P., Strohmayer, T. E., & Swank, J. H. 1998b, *ApJ*, 500, L171

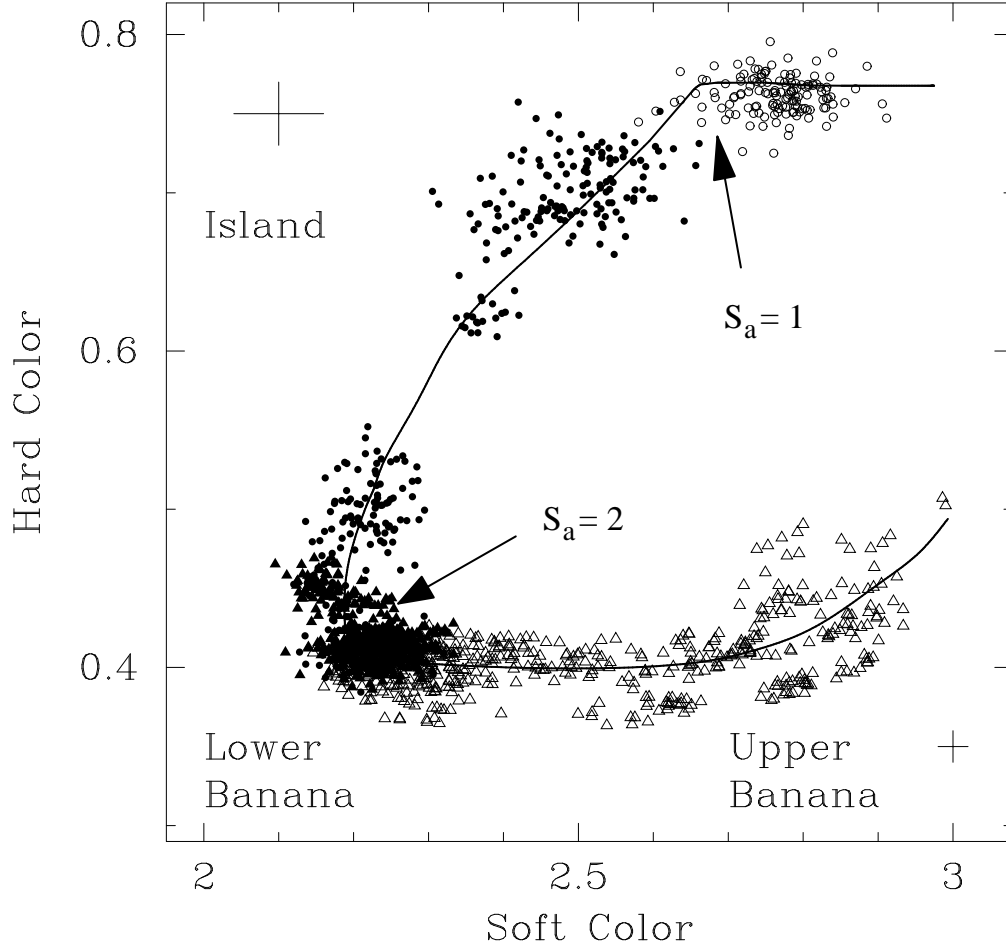


Fig. 1.— Color-Color diagram of 4U 1608–52. The soft and hard colors are defined as the ratio of count rates in the bands 3.5 – 6.4 keV and 2.0 – 3.5 keV, and 9.7 – 16.0 keV and 6.4 – 9.7 keV, respectively. The contribution of the background has been subtracted, but no dead-time correction was applied to the data (in this case the dead-time effects on the colors are less than 1 %). Each point represents 128 s of data. We show the typical error bars in the banana and the island states. Filled and open symbols indicate segments with and without kHz QPOs, respectively. We represent the island and banana states (defined on the basis of the low-frequency part of the power spectra) by circles and triangles, respectively. The curve shows the parametrization of the color-color diagram in terms of S_a (see text).

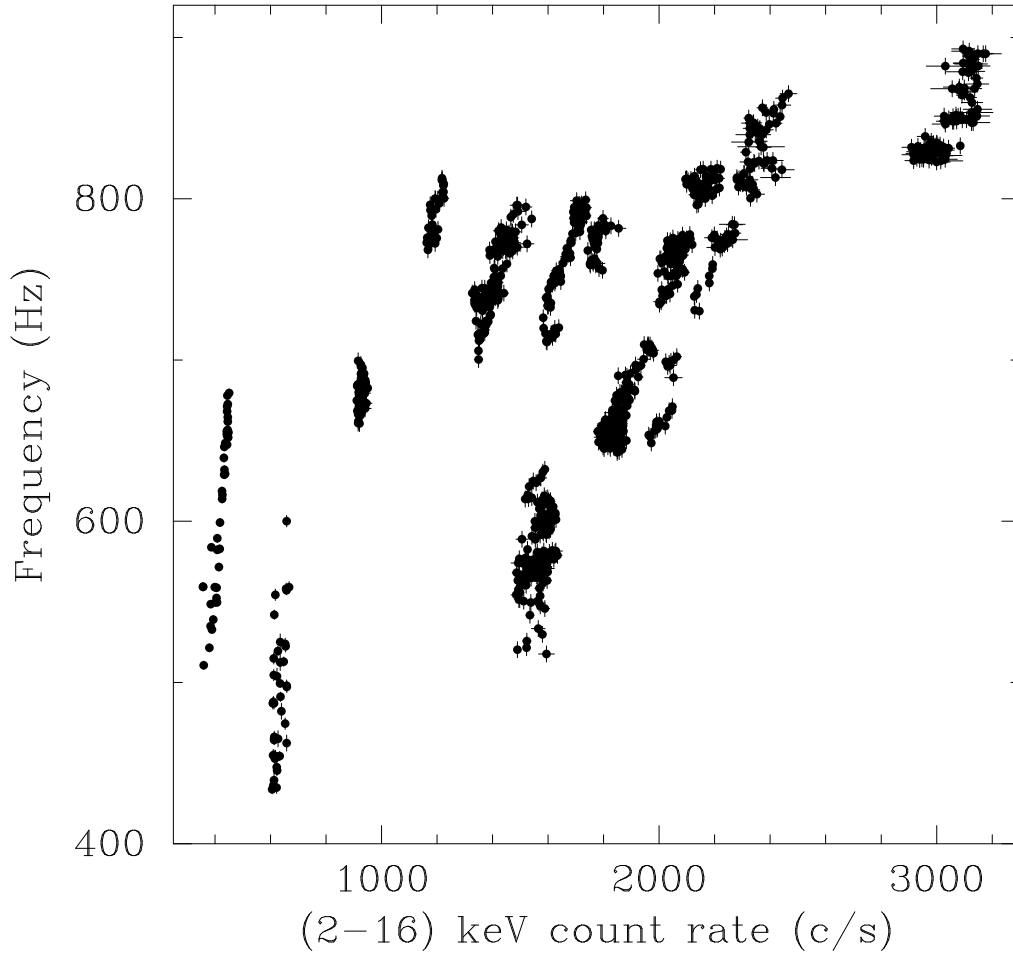


Fig. 2.— Relation between the frequency of the lower kHz QPO and the 2 – 16 keV count rate. The count rates have been corrected for background, and normalized to 5 detectors. Each point represents a 64-s segment (see text). We only include data where both kHz QPOs are detected simultaneously, so that we can unambiguously identify the lower kHz peak.

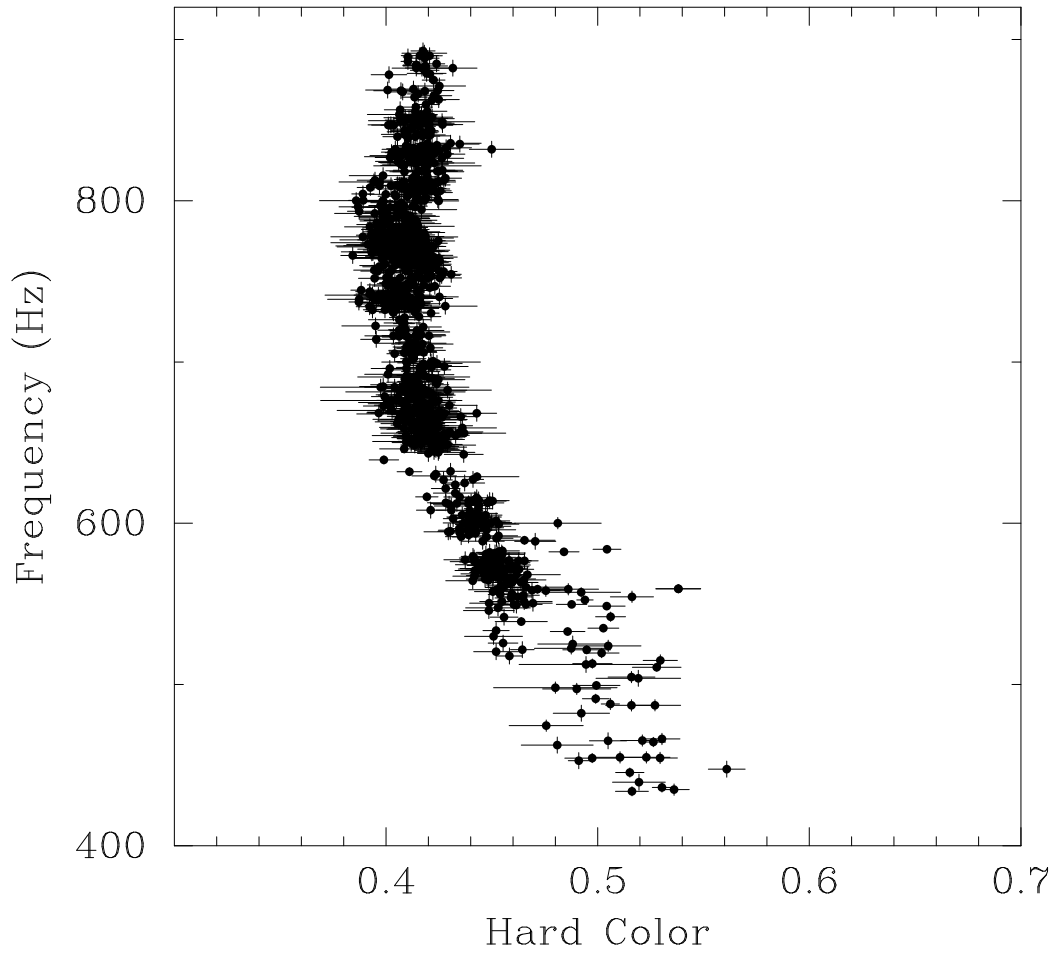


Fig. 3.— Relation between the frequency of the lower kHz QPO and the hard color (see Fig. 1), for the same segments shown in Figure 2.

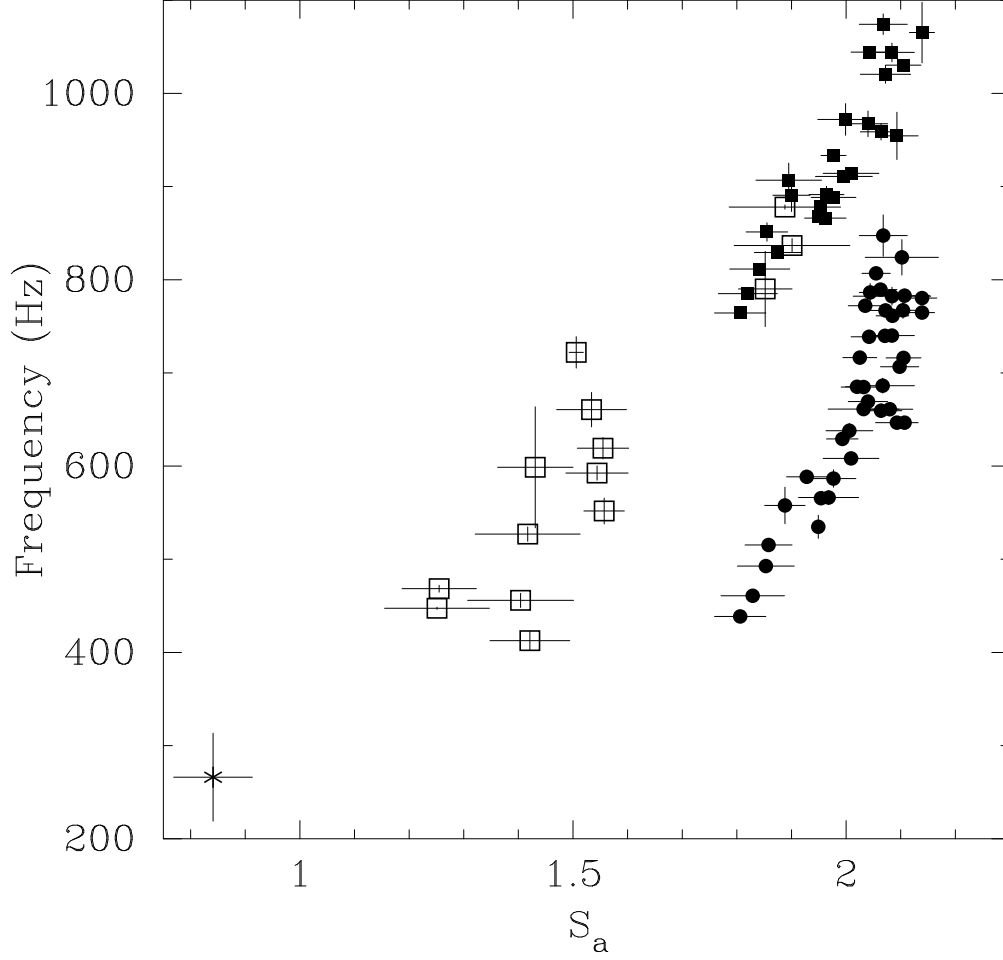


Fig. 4.— Diagram of the frequencies of the upper and lower kHz QPOs vs. the position of the source on the color-color diagram, as measured by S_a (see Fig. 1, and text). Circles and filled squares represent the lower and the upper kHz peak, respectively. Open squares represent segments where we only detected one of the kHz QPOs, and therefore we could not identify it as the upper or lower peak. The asterisk is one observation where we see a single QPO at a level of significance of 3σ only.